Sensor Control for Multi-target Tracking using Cauchy-Schwarz Divergence

Michael Beard*†, Ba-Tuong Vo†, Ba-Ngu Vo†, and Sanjeev Arulampalam‡
*Maritime Division, Defence Science and Technology Organisation, Rockingham, WA, Australia
†Department of Electrical and Computer Engineering, Curtin University, Bentley, WA, Australia
‡Maritime Division, Defence Science and Technology Organisation, Edinburgh, SA, Australia
michael.beard@dsto.defence.gov.au, ba-tuong.vo@curtin.edu.au,
ba-ngu.vo@curtin.edu.au,sanjeev.arulampalam@dsto.defence.gov.au

***Abstract*—In this paper, we propose a method for optimal stochastic sensor control, where the goal is to minimise the estimation error in multi-object tracking scenarios. Our approach is based on an information theoretic divergence measure between labelled random finite set densities. The multi-target posteriors are generalised labelled multi-Bernoulli (GLMB) densities, which do not permit closed form solutions for traditional information divergence measures such as Kullback-Leibler or Rényi. However, we demonstrate that the Cauchy-Schwarz divergence admits a closed form solution for GLMB densities, thus it can be used as a tractable objective function for multi-target sensor control. This is demonstrated with an application to sensor trajectory optimisation for bearings-only multi-target tracking.**

***Index Terms*—Multi-target sensor control, information theoretic control, generalised labelled multi-Bernoulli, Cauchy-Schwarz divergence, bearings-only trajectory optimisation**

I. Introduction

In most target tracking scenarios, the sensor can be controlled to perform various actions that may have a significant impact on the quality and information content of the measurement data, and therefore the estimation performance of the tracking system. Typically, such actions may include changing the position, orientation or motion of the sensor platform, which in turn affects the sensor's ability to detect, track, and identify objects in the scene. Often, the control decisions are driven by manual intervention, or by some deterministic control policy, which provides no guarantee of optimality. The goal of automatic sensor control is to determine the best control action to perform, based on some optimality criteria. This has the potential to improve tracking performance, by selecting the control actions in a manner that accounts for the current conditions.

This type of control problem can be formulated as a partially observable Markov decision process (POMDP) [1]–[4], which has also been referred to in the literature as a hidden Markov model multi-arm bandit problem [5]. In a POMDP, the multi-target dynamics is modelled as a Markov process, but only the posterior probability density function (pdf) of the multi-target state is known (conditioned on the past measurements), and the true underlying state is unknown. The measurements follow a known distribution, which is conditional on the multi-target state and the sensor control action. The benefit of performing a given action is expressed by a reward function, which characterises the objectives of the control system. Every time a decision is needed, the goal is to find the control action which maximises this reward function.

Within the POMDP framework, different types of reward functions may be used, depending on the objectives of the system. These generally fall into two categories; task-based criteria, and information-based criteria. Task-based control is useful in situations where the system objective can be formulated in terms of a single criterion (see for example [6]–[8]), but utilising this technique in the presence of multiple competing objectives is a challenging problem. On the other hand, information-based optimisation strives to quantify the overall information gained from executing a control action, therefore it does not suffer from the problem of competing objectives. Although information theoretic control may not lead to an optimal decision with respect to any particular task, the overall performance across multiple task objectives is likely to be superior [9]. It is for this reason that we focus our attention on information theoretic control in this paper.

The earliest use of information theoretic control for sensor management and state estimation appears to be the work of Hintz and McVey [10], where they investigate Shanon entropy in target tracking using Kalman filters. Since then, various information theoretic divergence measures such as the Kullback-Leibler (KL) divergence [11]–[13], and more generally the Rényi divergence [9], [12], [14]–[20], have been proposed for sensor management in single and multi-target tracking problems. In such problems, the expected divergence or information gain between the prior and posterior target densities is computed and used as the basis for selecting the optimal control action. While the KL and Rényi divergence based techniques have proven useful, a major limitation is their significant computational cost. In particular, except for certain special cases, these divergences cannot be computed analytically, thus requiring expensive approximations, typically based on Monte Carlo (MC) methods [17], [20], [21]. Other control algorithms motivated by the concept of the Fisher information matrix have also been proposed, for example, in problems such as sensor waveform selection [22], and trajectory planning [23]–[26].

An alternative information divergence measure is the Cauchy-Schwarz (CS) divergence [27], [28]. In [29], an analytical solution to the CS divergence between two mixtures of Poisson point processes was derived, with an application to range-only multi-target sensor control, based on the probability

hypothesis density (PHD) filter [30], [31]. The drawback of this approach is that it cannot be used in applications that require target tracks, since the PHD filter in principle does not produce tracks. Moreover, the PHD filter involves a drastic approximation to the multi-target posterior, which leads to highly uncertain cardinality estimates [32], [33].

In this paper, we consider the problem of sensor control for multi-target tracking via labelled random finite sets (RFS). In particular, we use a tracking algorithm called the generalised labelled multi-Bernoulli (GLMB) filter [34], [35], for which the result in [29] is not directly applicable. The key innovation of this paper is an analytic expression for the Cauchy-Schwarz divergence between two GLMB densities, which is used to construct the reward function for a POMDP-based sensor control scheme. This reward function accounts for target trajectories in a principled manner, which is not possible using unlabelled RFSs. Furthermore, the GLMB density provides a much more accurate approximation of the multi-target posterior, leading to improved estimation performance.

We have tested our proposed method by applying it in the context of a multi-target bearings-only tracking scenario, where the control algorithm is used to select an optimal course change for a moving sensor platform. In this type of scenario, the optimal choice of course change will be governed mainly by the effects of observability [36]–[38], as different course changes may lead to significantly different levels of observability for the targets.

II. Background: Multi-target Sensor Control

The goal of multi-target sensor control is to select the control action that, when executed, results in the lowest estimation error relative to all possible actions. It is generally not possible to compute this exactly, since calculating the true estimation error requires access to the scenario ground truth. It is often argued that a good substitute for minimising the estimation error, is to maximise the information gain, which can be quantified by the information divergence between the prior and posterior multi-object densities. Computing these densities requires a Bayesian multi-object filter, which we describe herein.

In multi-target tracking we represent the *multi-object state* as a finite set of single target states at each time k. The multi-object states $X_k \subset \mathbb{X}$ and *multi-object observations* $Z_k \subset \mathbb{Z}$ are modelled as random finite sets, and FISST is a framework for working with RFSs [39] based on a notion of integration/density that is consistent with point process theory [40]. The multi-object posterior density can be computed using the Bayes recursion.

At the previous time step $k-1$, the multi-object state is distributed according to a *multi-object density* $\pi_{k-1}(\cdot|Z_{1:k-1})$, where $Z_{1:k-1}$ is a collection of finite sets of measurements received up to time $k-1$. Each Z_k is assumed to be generated through a process of thinning of misdetected objects, Markov shifts of detected objects, and superposition of false measurements. The *multi-object prediction* to time k is given by the Chapman-Kolmogorov equation

$$\pi_{k|k-1}(X_k|Z_{1:k-1}) = \int f_{k|k-1}(X_k|X)\,\pi_{k-1}(X|Z_{1:k-1})\,\delta X, \tag{1}$$

where $f_{k|k-1}(X_k|X)$ is the multi-object transition kernel from time $k-1$ to time k, and the integral is the set integral,

$$\int f(X)\,\delta X = \sum_{i=0}^{\infty} \frac{1}{i!} \int_{\mathbb{X}^i} f(\{x_1,\ldots,x_i\})\,d(x_1,\ldots,x_i) \tag{2}$$

for any function f that takes $\mathcal{F}(\mathbb{X})$, the collection of all finite subsets of $\mathbb{X}$, to the real line. A new set of observations Z_k is received at time k, which is modelled by a *multi-object likelihood function* $g_k(Z_k|X_k)$. Thus the *multi-object posterior* at time k is given by Bayes rule

$$\pi_k(X_k|Z_{1:k}) = \frac{g_k(Z_k|X_k)\,\pi_{k|k-1}(X_k|Z_{1:k-1})}{\int g_k(Z_k|X)\,\pi_{k|k-1}(X|Z_{1:k-1})\,\delta X}. \tag{3}$$

Collectively, (1) and (3) are referred to as the *multi-object Bayes filter*. In general, computing the exact multi-object posterior is numerically intractable, and approximations are required to derive practical algorithms. Such algorithms include the probability hypothesis density (PHD) filter [30], the cardinalised PHD (CPHD) filter [32], the multi-object multi-Bernoulli (MeMBer) filter [39], [41], and the generalised labelled multi-Bernoulli (GLMB) filter [34], [35]. The GLMB filter has the distinct advantage that it produces labelled target state estimates. In the remainder of this section we briefly describe the main points of the GLMB filter, and for a more complete treatment the reader is referred to [34] and [35].

We begin by introducing some notation and definitions relating to labelled random finite sets. The multi-object exponential of a real valued function h raised to a set X is defined as $[h]^X \triangleq \prod_{x\in X} h(x)$, where $[h]^{\emptyset} = 1$, and the elements of X may be of any type such as scalars, vectors, or sets, provided that the function h takes an argument of that type. The generalised Kronecker delta function is defined as

$$\delta_Y(X) \triangleq \begin{cases} 1, & \text{if } X = Y \\ 0, & \text{otherwise} \end{cases} \tag{4}$$

where again, X and Y may be of any type, such as scalars, vectors, or sets. Finally, the set inclusion function is

$$1_Y(X) \triangleq \begin{cases} 1, & \text{if } X \subseteq Y \\ 0, & \text{otherwise} \end{cases}. \tag{5}$$

Definition 1. A *labelled RFS* with state space $\mathbb{X}$ and discrete label space $\mathbb{L}$, is an RFS on $\mathbb{X}\times\mathbb{L}$, such that the labels within each realisation are always distinct. That is, if $\mathcal{L}(\boldsymbol{X})$ is the set of unique labels in $\boldsymbol{X}$, and we define the distinct label indicator function as $\Delta(\boldsymbol{X}) = \delta_{|\boldsymbol{X}|}(|\mathcal{L}(\boldsymbol{X})|)$, then a labelled RFS $\boldsymbol{X}$ always satisfies $\Delta(\boldsymbol{X}) = 1$.

In general, we adopt the notational convention that labelled sets are expressed in bold upper case ($\boldsymbol{X}$), unlabelled sets in regular upper case (X), labelled vectors in bold lower case ($\boldsymbol{x}$), and unlabelled vectors in regular lower case (x).

Definition 2. A *generalised labelled multi-Bernoulli* (GLMB) RFS is a labeled RFS with state space $\mathbb{X}$ and discrete label space $\mathbb{L}$, which satisfies the probability distribution

$$\pi(\boldsymbol{X}) = \Delta(\boldsymbol{X}) \sum_{c\in\mathbb{C}} w^{(c)}(\mathcal{L}(\boldsymbol{X})) \left[p^{(c)}(\cdot)\right]^{\boldsymbol{X}} \tag{6}$$

where $\mathbb{C}$ is an arbitrary index set, $\sum_{L\subseteq\mathbb{L}}\sum_{c\in\mathbb{C}} w^{(c)}(L) = 1$, and $\int_{x\in\mathbb{X}} p^{(c)}(x,l)\,dx = 1$.

The GLMB, as defined above, has been shown to be a *conjugate prior* with respect to the standard multi-object likelihood, and closed under the Chapman-Kolmogorov equation for the standard multi-object transition [34] (i.e. the form of the density is retained through both prediction and update), which facilitates implementation of a Bayesian GLMB filter.

A. Prediction

Let $\boldsymbol{X}$ be the labelled RFS of objects at the current time with label space $\mathbb{L}$. A particular object $(x,l) \in \boldsymbol{X}$ has probability $p_S(x,l)$ of surviving to the next time with state (x_+,l_+) and probability density $f(x_+|x,l)\,\delta_l(l_+)$ (where $f(x_+|x,l)$ is the single target transition kernel), and probability, $q_S(x,l) = 1-p_S(x,l)$ of being terminated. Thus, the set $\boldsymbol{S}$ of surviving objects at the next time is distributed as

$$f_S(\boldsymbol{S}|\boldsymbol{X}) = \Delta(\boldsymbol{S})\,\Delta(\boldsymbol{X})\,1_{\mathcal{L}(\boldsymbol{X})}(\mathcal{L}(\boldsymbol{S}))\,[\Phi(\boldsymbol{S};\cdot)]^{\boldsymbol{X}} \tag{7}$$

where

$$\Phi(\boldsymbol{S};x,l) = \sum_{(x_+,l_+)\in\boldsymbol{S}} \delta_l(l_+)\,p_S(x,l)\,f(x_+|x,l) + \left(1-1_{\mathcal{L}(\boldsymbol{S})}(l)\right) q_S(x,l). \tag{8}$$

Now let $\boldsymbol{B}$ be the labeled RFS of newborn objects with label space $\mathbb{B}$, where $\mathbb{L}\cap\mathbb{B} = \emptyset$. To ensure that $\mathbb{L}$ and $\mathbb{B}$ are disjoint, we adopt a labelling scheme such that each new birth is labelled with a pair (t_b,l_b), where t_b is the current time and l_b is a unique index. Since the time changes from scan to scan, the space of birth labels is always disjoint from the space of surviving labels. Since the births have distinct labels, and assuming that their states are independent, we model $\boldsymbol{B}$ according to a labelled multi-Bernoulli distribution (LMB)

$$f_B(\boldsymbol{B}) = \Delta(\boldsymbol{B})\,w_B(\mathcal{L}(\boldsymbol{B}))\,[p_B(\cdot)]^{\boldsymbol{B}}. \tag{9}$$

where $p_B(\cdot,l)$ is the single target birth density, and $w_B(\cdot)$ is the birth weight (see Section IV-D of [34] for more details). We derive the prediction based on an LMB birth model, however, this can easily be extended to the case of a GLMB birth model. The overall multi-object state at the next time step is the union of survivals and new births, i.e. $\boldsymbol{X}_+ = \boldsymbol{S}\cup\boldsymbol{B}$. The label spaces $\mathbb{L}$ and $\mathbb{B}$ are disjoint, and the states of new born objects are independent of surviving objects, hence $\boldsymbol{S}$ and $\boldsymbol{B}$ are independent. It was shown in [34] that the multi-object transition can be expressed as

$$f(\boldsymbol{X}_+|\boldsymbol{X}) = f_S(\boldsymbol{X}_+\cap(\mathbb{X}\times\mathbb{L})\,|\boldsymbol{X})\,f_B(\boldsymbol{X}_+ - (\mathbb{X}\times\mathbb{L})), \tag{10}$$

and that a GLMB density of the form (6) is closed under the Chapman-Kolmogorov prediction (1) with the transition kernel defined by (10), where the predicted GLMB density is given by

$$\pi_+(\boldsymbol{X}_+) = \Delta(\boldsymbol{X}_+)\sum_{c\in\mathbb{C}} w_+^{(c)}(\mathcal{L}(\boldsymbol{X}_+))\left[p_+^{(c)}(\cdot)\right]^{\boldsymbol{X}_+} \tag{11}$$

where

$$w_+^{(c)}(L) = w_B(L-\mathbb{L})\,w_S^{(c)}(L\cap\mathbb{L}), \tag{12}$$

$$p_+^{(c)}(x,l) = 1_{\mathbb{L}}(l)\,p_S^{(c)}(x,l) + (1-1_{\mathbb{L}}(l))\,p_B(x,l), \tag{13}$$

$$p_S^{(c)}(x,l) = \frac{\left\langle p_S(\cdot,l)\,f(x|\cdot,l)\,,p^{(c)}(\cdot,l)\right\rangle}{\eta_S^{(c)}(l)}, \tag{14}$$

$$\eta_S^{(c)}(l) = \int\left\langle p_S(\cdot,l)\,f(x|\cdot,l)\,,p^{(c)}(\cdot,l)\right\rangle dx, \tag{15}$$

$$w_S^{(c)}(J) = \left[\eta_S^{(c)}\right]^J \sum_{I\subseteq\mathbb{L}} 1_I(J)\left[q_S^{(c)}\right]^{I-J} w^{(c)}(I), \tag{16}$$

$$q_S^{(c)}(l) = \left\langle q_S(x,l)\,,p^{(c)}(x,l)\right\rangle. \tag{17}$$

B. Update

Let $\boldsymbol{X}$ be the labelled RFS of objects that exist at the observation time. A particular object $(x,l)\in\boldsymbol{X}$ has probability $p_D(x,l)$ of generating a detection z with likelihood $g(z|x,l)$, and probability $q_D(x,l) = 1-p_D(x,l)$ of being misdetected. Let D be the set of target detections. Assuming the elements of D are conditionally independent, then D is a multi-Bernoulli RFS with existence and single-object density parameters given by the set $\{(p_D(x,l)\,,g(\cdot|x)) : (x,l)\in\boldsymbol{X}\}$, and we write its probability density as

$$\pi_D(D|\boldsymbol{X}) = \{(p_D(x,l)\,,g(\cdot|x)) : (x,l)\in\boldsymbol{X}\}(D). \tag{18}$$

Let K be the set of clutter observations, which are independent of the target detections. We model K as a Poisson RFS with intensity $\kappa(\cdot)$, hence K is distributed according to

$$\pi_K(K) = e^{-\langle\kappa,1\rangle}\kappa^K. \tag{19}$$

The overall multi-object observation is the union of target detections and clutter observations, i.e. $Z = D\cup K$. Since D and K are independent, the multi-object likelihood is

$$g(Z|\boldsymbol{X}) = \sum_{D\subseteq Z}\pi_D(D|\boldsymbol{X})\,\pi_K(Z-D). \tag{20}$$

As demonstrated in [39], this can be equivalently expressed as

$$g(Z|\boldsymbol{X}) = e^{-\langle\kappa,1\rangle}\kappa^K \sum_{\theta\in\Theta(\mathcal{L}(\boldsymbol{X}))}[\psi_Z(\cdot;\theta)]^{\boldsymbol{X}} \tag{21}$$

where $\Theta(\mathcal{L}(\boldsymbol{X}))$ is the set of all one-to-one mappings of labels in $\boldsymbol{X}$ to measurement indices in Z, (i.e. $\theta : \mathcal{L}(\boldsymbol{X}) \to \{0,1,...,|Z|\}$, such that $[\theta(i) = \theta(j) > 0] \Rightarrow [i=j]$), and $\psi_Z(\cdot;\theta)$ is

$$\psi_Z(x,l;\theta) = \begin{cases} \frac{p_D(x,l)g\left(z_{\theta(l)}|x,l\right)}{\kappa\left(z_{\theta(l)}\right)}, & \theta(l) > 0 \\ q_D(x,l)\,, & \theta(l) = 0 \end{cases} \tag{22}$$

It was demonstrated in [34] that a GLMB density of the form (6) is closed under the Bayes update (3) with likelihood function defined by (21), and the posterior density is given by

$$\pi(\boldsymbol{X}|Z) \tag{23}$$

$$= \Delta(\boldsymbol{X}) \sum_{c\in\mathbb{C}} \sum_{\theta\in\Theta(Z)} w_Z^{(c,\theta)}(\mathcal{L}(\boldsymbol{X})) \left[p^{(c,\theta)}(\cdot|Z)\right]^{\boldsymbol{X}}$$

where

$$w_Z^{(c,\theta)}(L) = \frac{w^{(c)}(L)\left[\eta_Z^{(c,\theta)}\right]^L}{\sum_{c\in\mathbb{C}}\sum_{J\subseteq\mathbb{L}}\sum_{\theta\in\Theta(Z)} w^{(c)}(J)\left[\eta_Z^{(c,\theta)}\right]^J}, \quad (24)$$

$$p^{(c,\theta)}(x,l|Z) = \frac{p^{(c)}(x,l)\,\psi_Z(x,l;\theta)}{\eta_Z^{(c,\theta)}(l)}, \quad (25)$$

$$\eta_Z^{(c,\theta)}(l) = \left\langle p^{(c)}(\cdot,l), \psi_Z(\cdot,l;\theta)\right\rangle. \quad (26)$$

C. Sensor Control

The problem remains that at the time when we wish to perform a control action, we have no knowledge of the posterior density that would arise from taking that action. Since the true information divergence is not yet available, the expectation of the information divergence with respect to all possible future measurements is used [20], [42]. More precicely, let us begin by defining the following notation

- $\pi_k(\cdot|Z_{1:k})$ is the multi-object GLMB posterior at time k,
- C_k is the set of allowable control actions at time k,
- H is the horizon length for calculation of the reward,
- $\pi_{k+H}(\cdot|Z_{1:k})$ is the multi-object GLMB prediction from time k to $k+H$,
- $Z_{k+1:k+H}(c)$ is the collection of measurement sets that would be observed from times $k+1$ up to $k+H$, if control action $c \in C_k$ was executed at time k.

The optimal control action is given by maximising the expected value of a reward function $\mathcal{R}_{k+H}(\cdot)$ over the set of allowable actions,

$$c_{opt} = \arg\max_{c\in C_k} \mathbb{E}\left[\mathcal{R}_{k+H}(c)\right], \quad (27)$$

where the reward function is given by some form of information divergence $D(\cdot,\cdot)$ between the predicted and posterior multi-object densities,

$$\mathcal{R}_{k+H}(c) = D\left(\pi_{k+H}(\boldsymbol{X}|Z_{1:k}), \pi_{k+H}(\boldsymbol{X}|Z_{1:k}, Z_{k+1:k+H}(c))\right). \quad (28)$$

and the expectation is taken with respect to the future measurement sets $Z_{k+1:k+H}(c)$. A further problem is that calculation of the divergence (as well as its expectation) is generally intractable, which presents a major challenge in the development of tractable sensor control algorithms. A solution to this problem is proposed in the following section.

III. Cauchy-Schwarz Divergence for GLMB Densities

The most commonly used measures of information gain are the Kullback-Leibler divergence, and more generally, the Rényi divergence. However, their form precludes analytical solutions for all but very simple probability density functions, and in the case of more complicated pdfs (such as the GLMB), one must resort to approximate numerical methods. In this section we show that the Cauchy-Schwarz divergence has a mathematical form which is more amenable to closed form solution, and in particular, a closed form can be obtained for GLMB densities, in the case where the individual target densities are Gaussian mixtures.

In the context of random finite sets, the Csiszár-Morimoto divergence (of which Kullback-Leibler and Rényi are special cases), can be formulated by replacing the standard (Lebesque) integral with the set or FISST integral [39]. However, unlike the Csiszár-Morimoto divergence, the Cauchy-Schwarz divergence cannot be extended to FISST densities by simply replacing the standard integral with the set integral. To see this, consider the naive inner product between two FISST densities ϕ and φ via the set integral:

$$\langle\phi,\varphi\rangle = \int \phi(X)\varphi(X)\delta X \quad (29)$$
$$= \sum_{i=0}^{\infty} \frac{1}{i!}\int_{\mathbb{X}^i} \phi(\{x_1,...,x_i\})\varphi(\{x_1,...,x_i\})d(x_1,...,x_i).$$

Note that the FISST density is not a probability density, and the functions $\phi(\{x_1,...,x_i\})$ and $\varphi(\{x_1,...,x_i\})$ each have units of K^{-i}, and $d(x_1,...,x_i)$ has units of K, where K is the unit of hyper-volume in $\mathbb{X}$. Since the i-th term in the above sum has units of K^{-i}, the sum is not meaningful because the terms cannot be added together due to a unit mismatch, e.g. if $K = m^3$, then the first term is unitless, the second term is in m^{-3}, the third term is in m^{-6}, and so on.

A. Cauchy-Schwarz Divergence for RFS

To define the Cauchy-Schwarz (CS) divergence for RFS densities, we need to resort to the Lebesque integral. The probability density of an RFS can be defined with respect to the reference measure μ given by [40]

$$\mu(\mathcal{T}) = \sum_{i=0}^{\infty} \frac{1}{i!K^i}\int_{\mathbb{X}^i} 1_{\mathcal{T}}(\{x_1,...,x_i\})d(x_1,...,x_i) \quad (30)$$

for any (measurable) subset $\mathcal{T}$ of $\mathcal{F}(\mathbb{X})$, where $\mathbb{X}^i$ denotes the i^{th}-fold Cartesian product of $\mathbb{X}$, with the convention $\mathbb{X}^0 = \{\emptyset\}$, and the integral over $\mathbb{X}^0$ is $1_{\mathcal{T}}(\emptyset)$. The measure μ is analogous to the Lebesque measure on $\mathbb{X}$ (indeed it is the unnormalized distribution of a Poisson point process with unit intensity $u = \frac{1}{K}$ when the state space $\mathbb{X}$ is bounded). Moreover, it was shown in [40] that for this choice of reference measure, the Lebesque integral of a function $f : \mathcal{F}(\mathbb{X}) \to \mathbb{R}$, given by

$$\int f(X)\mu(dX) = \sum_{i=0}^{\infty} \frac{1}{i!K^i}\int_{\mathbb{X}^i} f(\{x_1,...,x_i\})d(x_1,...,x_i), \quad (31)$$

is equivalent to Mahler's set integral [39]. Note that the reference measure μ, and the integrand f are all dimensionless.

Using the Lebesque integral we can define the inner product $\langle f,g\rangle_\mu \triangleq \int f(X)g(X)\mu(dX)$, and corresponding norm $\|f\|_\mu \triangleq \sqrt{\langle f,f\rangle_\mu}$. Such forms for the inner product and norm are well-defined because the densities f and g, as well as the reference measure μ, are all unitless.

Definition 3. The Cauchy-Schwarz divergence between the probability densities f and g of two point processes with

respect to the reference measure μ is defined by

$$D_{CS}(f,g) = -\ln \frac{\langle f,g\rangle_\mu}{\|f\|_\mu \|g\|_\mu}. \tag{32}$$

It was shown in [29] that *the CS divergence of two Poisson RFSs equals half the squared distance between their PHDs.* Moreover, an analytic expression for the CS divergence between two mixtures of Poisson RFSs was derived.

The above definition of the Cauchy-Schwarz divergence can be equivalently expressed in terms of set integrals as follows. Let ϕ and φ denote the FISST densities of the respective point processes. Using the relationship between the FISST density and the Radon-Nikodym derivative in [40], the corresponding probability densities relative to μ are given by $f(X) = K^{|X|}\phi(X)$ and $g(X) = K^{|X|}\varphi(X)$. Since

$$\begin{aligned}
&\langle f,g\rangle_\mu \\
&= \sum_{i=0}^{\infty} \frac{1}{i!} \int K^i \phi(\{x_1,...,x_i\})\varphi(\{x_1,...,x_i\}) d(x_1,...,x_i) \\
&= \int K^{|X|}\phi(X)\varphi(X)\delta X,
\end{aligned} \tag{33}$$

the Cauchy-Schwarz divergence can be written in terms of the set integral as follows

$$D_{CS}(\phi,\varphi) = -\ln\left(\frac{\int K^{|X|}\phi(X)\varphi(X)\delta X}{\sqrt{\int K^{|X|}\phi^2(X)\delta X \int K^{|X|}\varphi^2(X)\delta X}}\right). \tag{34}$$

Remark: Note that it is easy to show that a change in the unit of measurement K, does not change the value of the integrals, and hence the CS divergence is in fact independent of K.

B. Cauchy-Schwarz Divergence for GLMB

Using the definition in (34), we show that the CS divergence between two GLMBs can be written in closed form.

Proposition 4. *For two generalised labelled multi-Bernoulli densities defined by*

$$\phi(\boldsymbol{X}) = \Delta(\boldsymbol{X}) \sum_{c\in\mathbb{C}} w_\phi^{(c)}(\mathcal{L}(\boldsymbol{X})) \left[p_\phi^{(c)}(\cdot)\right]^{\boldsymbol{X}}, \tag{35}$$

$$\psi(\boldsymbol{X}) = \Delta(\boldsymbol{X}) \sum_{d\in\mathbb{D}} w_\psi^{(d)}(\mathcal{L}(\boldsymbol{X})) \left[p_\psi^{(d)}(\cdot)\right]^{\boldsymbol{X}}, \tag{36}$$

the Cauchy-Schwarz divergence between ϕ and ψ is given by

$$D_{CS}(\phi,\psi) = -\ln\left(\frac{\zeta(\phi,\psi)}{\sqrt{\zeta(\phi,\phi)\,\zeta(\psi,\psi)}}\right), \tag{37}$$

where

$$\begin{aligned}
\zeta(\phi,\psi) = &\sum_{L\subseteq\mathbb{L}} \sum_{c\in\mathbb{C}} \sum_{d\in\mathbb{D}} w_\phi^{(c)}(L)\, w_\psi^{(d)}(L) \\
&\times \left[K \int p_\phi^{(c)}(x,\cdot)\, p_\psi^{(d)}(x,\cdot)\, dx\right]^L.
\end{aligned} \tag{38}$$

Proof: If $\phi(\boldsymbol{X})$ and $\psi(\boldsymbol{X})$ are two GLMB densities defined by (35) and (36), the set integral can be expressed as

$$\begin{aligned}
&\int K^{|\boldsymbol{X}|}\phi(\boldsymbol{X})\,\psi(\boldsymbol{X})\,\delta\boldsymbol{X} \\
&= \int K^{|\boldsymbol{X}|}\Delta(\boldsymbol{X}) \sum_{c\in\mathbb{C}} w_\phi^{(c)}(\mathcal{L}(\boldsymbol{X})) \left[p_\phi^{(c)}(\cdot)\right]^{\boldsymbol{X}} \\
&\quad\times \sum_{d\in\mathbb{D}} w_\psi^{(d)}(\mathcal{L}(\boldsymbol{X})) \left[p_\psi^{(d)}(\cdot)\right]^{\boldsymbol{X}} \delta\boldsymbol{X} \\
&= \int \Delta(\boldsymbol{X}) \sum_{c\in\mathbb{C}} \sum_{d\in\mathbb{D}} w_\phi^{(c)}(\mathcal{L}(\boldsymbol{X}))\, w_\psi^{(d)}(\mathcal{L}(\boldsymbol{X})) \\
&\quad\times K^{|\mathcal{L}(\boldsymbol{X})|} \left[p_\phi^{(c)}(\cdot)\, p_\psi^{(d)}(\cdot)\right]^{\boldsymbol{X}} \delta\boldsymbol{X} \\
&= \sum_{L\subseteq\mathbb{L}} \sum_{c\in\mathbb{C}} \sum_{d\in\mathbb{D}} w_\phi^{(c)}(L)\, w_\psi^{(d)}(L) \\
&\quad\times \left[K \int p_\phi^{(c)}(x,\cdot)\, p_\psi^{(d)}(x,\cdot)\, dx\right]^L,
\end{aligned} \tag{39}$$

where the last line is obtained by making use of Lemma 3 in [34]. Substituting (39) into (34), we are left with (37), with the inner product $\zeta(\cdot,\cdot)$ defined by (38). ■

We now apply the same result to the case of two δ-GLMB densities, which leads to a tractable closed form solution that can be applied in practice. Let the two densities be δ-GLMBs as follows

$$\phi(\boldsymbol{X}) = \Delta(\boldsymbol{X}) \sum_{\substack{(I,\alpha)\in \\ \mathcal{F}(\mathbb{L})\times\Xi}} w_\phi^{(I,\alpha)} \delta_I(\mathcal{L}(\boldsymbol{X})) \left[p_\phi^{(\alpha)}(\cdot)\right]^{\boldsymbol{X}}, \tag{40}$$

$$\psi(\boldsymbol{X}) = \Delta(\boldsymbol{X}) \sum_{\substack{(J,\beta)\in \\ \mathcal{F}(\mathbb{L})\times\Omega}} w_\psi^{(J,\beta)} \delta_J(\mathcal{L}(\boldsymbol{X})) \left[p_\psi^{(\beta)}(\cdot)\right]^{\boldsymbol{X}}, \tag{41}$$

where Ξ and Ω are spaces of measurement-to-target association histories. This leads to the following inner product

$$\begin{aligned}
\zeta(\phi,\psi) = &\sum_{L\subseteq\mathbb{L}} \sum_{\substack{(I,\alpha)\in \\ \mathcal{F}(\mathbb{L})\times\Xi}} \sum_{\substack{(J,\beta)\in \\ \mathcal{F}(\mathbb{L})\times\Omega}} w_\phi^{(I,\alpha)} w_\psi^{(J,\beta)} \delta_I(L)\,\delta_J(L) \\
&\times \left[K \int p_\phi^{(\alpha)}(x,\cdot)\, p_\psi^{(\beta)}(x,\cdot)\, dx\right]^L.
\end{aligned} \tag{42}$$

Notice that the product of the two delta functions inside the summation in (42) means that the only non-zero terms are those which satisfy $I = J = L$, i.e. the summation is over all pairs of components with matching target labels, which can be expressed as follows

$$\begin{aligned}
\zeta(\phi,\psi) = &\sum_{L\subseteq\mathbb{L}} \sum_{\substack{(L,\alpha) \\ \in\mathcal{F}(\mathbb{X})\times\Xi}} \sum_{\substack{(L,\beta)\in \\ \mathcal{F}(\mathbb{L})\times\Omega}} w_\phi^{(L,\alpha)} w_\psi^{(L,\beta)} \\
&\times \left[K \int p_\phi^{(\alpha)}(x,\cdot)\, p_\psi^{(\beta)}(x,\cdot)\, dx\right]^L.
\end{aligned} \tag{43}$$

Thus if the inner product between two single target densities is computable, which is the case for Gaussian mixtures [28], then the Cauchy-Schwarz divergence between two δ-GLMB densities can be evaluated tractably in closed form. It is worth noting here that if two δ-GLMB's contain no components with matching labels, then the inner product (43) will evaluate to zero, leading to a Cauchy-Schwarz divergence of infinity. This is an intuitive result, because if there are no matching sets of labels, there is effectively zero overlap between the two densities, which results in the maximum possible divergence.

C. Computation of Cauchy-Schwarz based Reward

Having established an analytic expression for the Cauchy-Schwarz divergence between two GLMBs, we now proceed to present a strategy for computing the reward function.

Recall from (27) that we need to compute the expected value of the divergence between the predicted and posterior GLMB densities. This does not have a closed form solution, so in order to approximate this expectation, we use the following procedure.

1) Compute the predicted density at the end of the control horizon $\pi_{k+H}(\boldsymbol{X}|Z_{1:k})$, by carrying out repeated prediction steps of the GLMB filter, without target birth or death, from time k up to time $k+H$.
2) Draw a set of N multi-target samples from $\pi_k(\boldsymbol{X}|Z_{1:k})$, which we denote as $\mathcal{S} = \left\{\boldsymbol{X}^{(1)}, \ldots, \boldsymbol{X}^{(N)}\right\}$.
3) For each $\boldsymbol{X}^{(i)} \in \mathcal{S}$, generate future sets of idealised measurements $\tilde{Z}_{k+1:k+H}\left(c, \boldsymbol{X}^{(i)}\right)$, i.e. simulate measurements based on the predicted future trajectories in sample $\boldsymbol{X}^{(i)}$, with zero clutter, zero process noise, zero measurement noise, and unity detection probability.
4) Compute the reward conditioned on each multi-target sample in $\mathcal{S}$. To do this, we initialise a GLMB filter at time k with density $\pi_k(\boldsymbol{X}|Z_{1:k})$, then run the GLMB filter recursion forward up to time $k+H$ using the measurements $\tilde{Z}_{k+1:k+H}\left(c, \boldsymbol{X}^{(i)}\right)$. This gives us the posterior density $\pi_{k+H}\left(\boldsymbol{X}|Z_{1:k}, \tilde{Z}_{k+1:k+H}\left(c, \boldsymbol{X}^{(i)}\right)\right)$, which we then use to compute the following reward for sample i,
$$\mathcal{R}^{(i)}_{k+H}(c) = D_{CS}\Big(\pi_{k+H}(\boldsymbol{X}|Z_{1:k}), \quad \pi_{k+H}\Big(\boldsymbol{X}|Z_{1:k}, \tilde{Z}_{k+1:k+H}\left(c, \boldsymbol{X}^{(i)}\right)\Big)\Big). \tag{44}$$
5) Having computed (44) for all samples in $\mathcal{S}$, the expectation of the reward is approximated as the mean of the sample rewards,
$$\mathbb{E}\left[\mathcal{R}_{k+H}(c)\right] \approx \frac{1}{N}\sum_{i=1}^{N} \mathcal{R}^{(i)}_{k+H}(c). \tag{45}$$

In the above method, steps 1 and 2 need only be carried out once, since the predicted density at the control horizon does not depend on the control action, and the same set of multi-target samples should be used in the reward calculation for each action. Therefore, we repeat steps 3-5 for each $c \in C_k$, after which we select and execute the control action which produced the highest expected reward as computed by (45).

IV. Simulation Results

In this section we apply the sensor control strategy described in the previous section, to the problem of observer trajectory optimisation for single-sensor bearings-only tracking. This type of problem has been studied before in [17], [23]–[25], [43]–[46], however, these have been limited to the case of a single target. The method proposed in this paper allows us to deal with the more general case where multiple targets may be present in the scene.

The targets are modelled using 2D Cartesian position and velocity vectors $x = \begin{bmatrix} p_x & \dot{p}_x & p_y & \dot{p}_y \end{bmatrix}^T$, and are assumed to move according to the following discrete white noise acceleration model,

$$x_{k+1} = Fx_k + \Gamma v_k, \tag{46}$$
$$F = \begin{bmatrix} 1 & T \\ 0 & 1 \end{bmatrix} \otimes I_2, \qquad \Gamma = \begin{bmatrix} T^2/2 \\ T \end{bmatrix} \otimes I_2$$

where T is the sampling period, $v_k \sim \mathcal{N}(0, Q)$ is a 2×1 independent and identically distributed Gaussian process noise vector with $Q = \sigma_v^2 I_2$, where σ_v is the standard deviation of the target acceleration. The sensor measures only target bearings, where the measurement corresponding to target t is modelled according to

$$z_k^{(t)} = h\left(x_k^{(t)}, u_k\right) + w_k \tag{47}$$

where $x_k^{(t)}$ is the true state of target t at time k, $u_k = \begin{bmatrix} p_{x,k}^{(s)} & p_{y,k}^{(s)} \end{bmatrix}$ is the sensor position at time k, $w_k \sim \mathcal{N}\left(0, \sigma_w^2\right)$ is scalar Gaussian measurement noise, and the measurement function h is given by

$$h\left(x_k^{(t)}, u_k\right) = \arctan\left(\frac{p_{y,k}^{(t)} - p_{y,k}^{(s)}}{p_{x,k}^{(t)} - p_{y,k}^{(s)}}\right). \tag{48}$$

The sensor platform moves with constant velocity, but undergoes course changes at certain pre-specified times, in an attempt to improve the observability of the targets being tracked. Conducting sensor manoeuvres is very important in bearings-only tracking, as they are necessary to establish target observability [36]–[38], and therefore play a pivotal role in determining the tracking performance.

The test scenario consists of three targets, which enter the scene between time 0 and 200. The sensor platform carries out a pre-determined course change at time 400, in order to improve the track estimates prior to executing the control algorithm. At time 800, the control algorithm is executed to compute the optimal course change at that time. The computed course change is then carried out, and the sensor platform remains on that course until the end of the scenario at time 1600. The sensor generates measurements with a sampling period of $T = 2$s, and the measurement noise is $\sigma_w = 0.5°$. The target-observer geometry is shown in Figure 1.

In computing the optimal course change at time 800, the idealised measurements are generated over a horizon length of $H = 10$, with sampling period $T = 40$s, which means that the control algorithm is looking ahead by 400s (up to time 1200s). The space of control actions is discretised at an interval of 20°, i.e. the set of allowed course changes is $C = \{-180°, -160°, \ldots, 0°, \ldots, 160°, 180°\}$, and the number of samples used to compute the expected reward is $N = 50$.

To establish the effectiveness of the proposed control method, we need to determine the true optimal control action for this scenario to use as a benchmark. We have done this by carrying out 200 Monte Carlo runs of the entire scenario, under each possible control action. We then calculate the average optimal sub-pattern assignment (OSPA) distance [47] at the horizon time (1200s), and plot the result as a function of

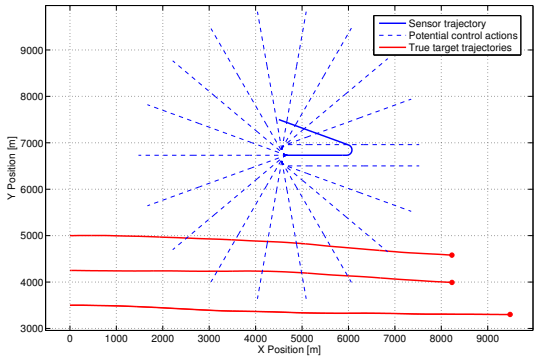

Figure 1. Target-observer geometry. The solid blue line is the sensor trajectory up to time 800. The trajectory after time 800 is determined by the control algorithm, which considers all the possible control actions shown by the dashed blue lines. Note that once the algorithm decides upon a new course, it remains fixed until the end of the scenario.

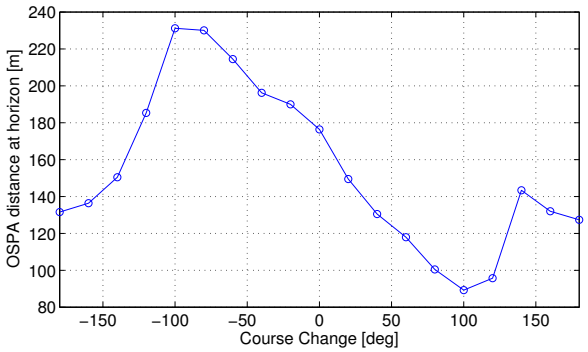

Figure 2. Course change vs average OSPA, evaluated at the control horizon time of 1200s.

course change. The course change with the lowest OSPA at the horizon time can be considered as the true optimal decision, which is unknown to the control algorithm. If the algorithm is working well, we should expect it to make the true optimal decision in the majority of runs. The result for this scenario is shown in Figure 2, from which we observe that the true optimal course change is 100°.

To test the control algorithm, we perform 200 Monte Carlo runs of the scenario, in which the algorithm decides on the course change at time 800s. Firstly, we show the tracking output of a typical run in Figure 3, in which the algorithm has

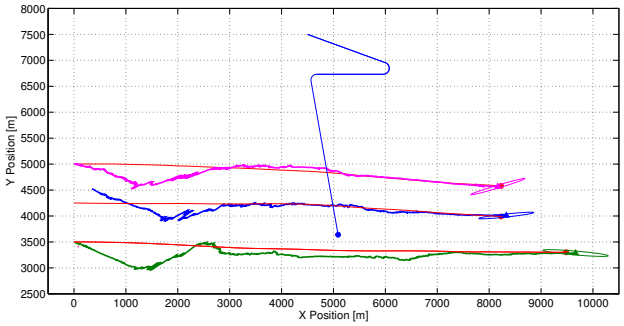

Figure 3. Track output from a typical run of the control scenario.

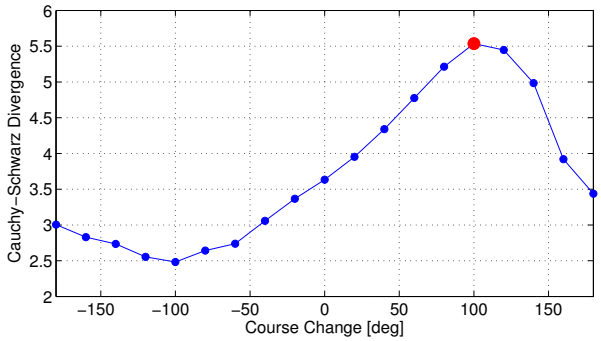

Figure 4. Reward curve generated by the control algorithm for a typical run.

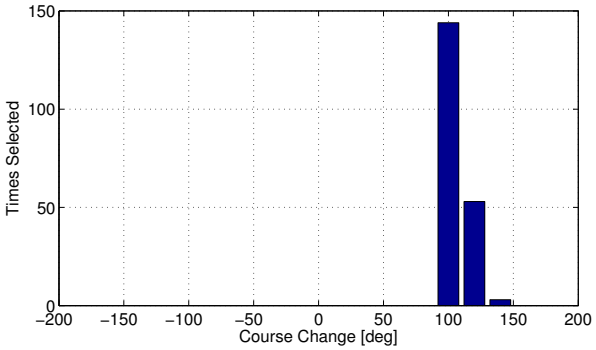

Figure 5. Frequency of selection for each control action across 200 Monte Carlo runs.

correctly chosen the optimal manoeuvre. The reward curve for this run is shown in Figure 4, in which we plot the expected value of the Cauchy-Schwarz divergence as a function of course change. We can see from Figure 4, that the shape of the reward curve exhibits an inverse relationship with the OSPA curve in Figure 2. This is expected, as the control actions that result in lower OSPA values should correspond to those with higher rewards, and vice-versa.

To demonstrate the overall performance of the control algorithm on this scenario, Figure 5 shows a histogram of the number of times that each possible manoeuvre was selected across the 200 Monte Carlo runs. The true optimal manoeuvre of 100° was selected on almost three-quarters of the runs, and the second-best manoeuvre of 120° was selected on most of the remaining runs. This result shows that the Cauchy-Schwarz divergence is capable of identifying the optimal control action with a good degree of reliability.

V. Conclusion

In this paper we have proposed a new method for multi-target sensor control based on maximising the expected Cauchy-Schwarz divergence between generalised labelled multi-Bernoulli densities. The Cauchy-Schwarz divergence between two known GLMB densities can be computed in closed form, which leads to a more efficient implementation than other divergence measures, which require the use of numerical integration methods. The proposed algorithm was shown to be effective in finding the optimal course change in a simulated

bearings-only multi-target tracking scenario. A possibility for future research in this area may involve applying this technique to non-standard sensor models, for example using the method in [48], which presented a GLMB filter for tracking in the presence of merged measurements.

REFERENCES

[1] D. P. Bertsakas, *Dynamic Programming and Optimal Control*, Belmont:Athena Scientific, 1995.

[2] G. E. Monahan, "State of the art - A survey of partially observable Markov decision processes: Theory, models and algorithms," *Management Science*, vol. 28, no. 1, 1982.

[3] W. S. Lovejoy, "A survey of algorithmic methods for partially observed Markov decision processes," *Annals of Operations Research*, vol. 28, pp. 47-66, 1991.

[4] V. Krishnamurthy, "Algorithms for optimal scheduling and management of hidden Markov model sensors," *IEEE Trans. Signal Process*., vol. 50, no. 6, June 2002.

[5] V. Krishnamurthy, R. J. Evans, "Hidden Markov model multiarm bandits: A methodology for beam scheduling in multitarget tracking," *IEEE Trans. Signal Process*., vol. 49, no. 12, Dec. 2001.

[6] R. Mahler, T. R. Zajic, "Probabilistic objective functions for sensor management," *Proc. SPIE Signal Processing, Sensor Fusion, and Target Recognition XIII*, vol. 5429, pp. 233–244, Aug. 2004.

[7] A. Gostar, R. Hoseinnezhad, A. Bab-Hadiashar, "Robust multi-Bernoulli sensor selection for multi-target tracking in sensor networks," *IEEE Signal Process. Lett*., vol. 20, no. 12, pp. 1167–1170, September 2013.

[8] A. K. Gostar, R. Hoseinnezhad, A. Bab-Hadiashar, "Sensor control for multi-object tracking using labeled multi-Bernoulli filter," *Proc. 17th Int. Conf. Information Fusion*, Salamanca, Spain, July 2014.

[9] C. Kreucher, A. O. Hero, K. Kastella, "A comparison of task driven and information driven sensor management for target tracking," *Proc. 44th IEEE Conf. Decision and Control, and 2005 European Control Conf. (CDC-ECC'05),* Dec. 2005.

[10] K. J. Hintz, E. S. McVey, "Multi-process constrained estimation," *IEEE Trans. Syst., Man, Cybern*., Syst., vol. 21, no. 1, pp. 237-244, January 1991.

[11] R. Mahler, "Global optimal sensor allocation," *Proc. Ninth National Symp. on Sensor Fusion*, vol. 1, pp. 167-172, 1996.

[12] J. M. Aughenbaugh, B. R La Cour, "Metric selection for information theoretic sensor management," *Proc. 11th Int. Conf. Information Fusion*, Cologne, Germany, July 2008.

[13] K. Kastella, "Discrimination gain to optimize detection and classification," *IEEE Transactions on Systems, Man & Cybernetics - Part A: Systems and Humans*, vol. 27, vo. 1, pp. 112-116, Jan. 1997.

[14] A. Rényi, "On measures of entropy and information", *Proc. 4th Berkeley Symp. Math. Stat. and Prob.*, vol. 1, pp. 547-561, 1961.

[15] T. Hanselmann, M. Morelande, B. Moran, P. Sarunic, "Sensor scheduling for multiple target tracking and detection using passive measurements," *Proc. 11th Int. Conf. Information Fusion*, Cologne, Germany, July 2008.

[16] C. M. Kreucher, A. O. Hero III, K. D. Kastella, M. R Morelande, "An information-based approach to sensor management in large dynamic networks," *Proc. IEEE*, vol. 95, no. 5, pp. 978-999, May 2007.

[17] B. Ristic, S. Arulampalam, "Bernoulli particle filter with observer control for bearings-only tracking in clutter," *IEEE Trans. Aerosp. Electron. Syst*., vol. 48, no. 3, pp. 2405-2415, July 2012.

[18] H. G. Hoang, B.-T. Vo, "Sensor management for multi-target tracking via multi-Bernoulli filtering," *Automatica*, vol. 50, no. 4, pp. 1135–1142, April 2014.

[19] A. O. Hero III, C. M. Kreucher, D. Blatt, "Information theoretic approaches to sensor management," *Foundations and applications of sensor management*, pp. 33-57, Springer US, 2008.

[20] B. Ristic and B.-N. Vo, "Sensor control for multi-object state-space estimation using random finite sets," *Automatica*, vol. 46, no. 11, pp. 1812 – 1818, Nov. 2010.

[21] B. Ristic, B.-N. Vo, D. Clark, "A note on the reward function for PHD filters with sensor control," *IEEE Trans. Aerosp. Electron. Syst*., vol. 47, no. 2, pp. 1521-1529, Apr. 2011.

[22] D. J. Kershaw, R. J. Evans, "Optimal Waveform Selection for Target Tracking," *IEEE Trans. Inf. Theory*, vol. 40, no. 5, pp. 1536–1550, Sep. 1994.

[23] J. M. Passerieux, V. van Cappel, "Optimal observer maneuver for bearings-only tracking," *IEEE Trans. Aerosp. Electron. Syst*., vol. 34, no. 3, pp. 777-788, July 1998.

[24] Y. Oshman, P. Davidson, "Optimization of observer trajectories for bearings-only target localization," *IEEE Trans. Aerosp. Electron. Syst*., vol. 35, no. 3, pp. 892-902, July 1999.

[25] J.-P. Le Cadre, S. Laurent-Michel, "Optimizing the receiver maneuvers for bearings-only tracking," *Automatica*, vol. 35, pp. 591-606, April 1999.

[26] R. Tharmarasa, T. Kirubarajan. M. L. Hernandez, A. Sinha, "PCRLB-based multisensor array management for multitarget tracking," *IEEE Trans. Aerosp. Electron. Syst*., vol. 43, no. 2, pp. 539-555, Apr. 2007.

[27] R. Jenssen, J. C. Principe, D. Erdogmus, and T. Eltoft, "The Cauchy–Schwarz divergence and Parzen windowing: Connections to graph theory and Mercer kernels," *Journal of the Franklin Institute*, vol. 343, no. 6, pp. 614–629, Sep. 2006.

[28] K. Kampa, E. Hasanbelliu, J. C. Principe, "Closed form Cauchy-Schwarz PDF divergence for mixture of Gaussians," *Proc. IEEE Int. Joint Conf. on Neural Networks (IJCNN 2011)*, San Jose, California, USA, pp. 2578–2585, Aug. 2011.

[29] H. G. Hoang, B.-N. Vo, B.-T. Vo, R. Mahler, "The Cauchy-Schwarz divergence for Poisson point processes," arXiv preprint, arXiv:1312.6224, July 2014.

[30] R. Mahler, "Multitarget Bayes filtering via first-order multitarget moments", *IEEE Trans. Aerosp. Elecron. Syst*., vol. 39, no. 4, pp. 1152-1178, Oct. 2003.

[31] B.-N. Vo, W.-K. Ma, "The Gaussian mixture probability hypothesis density filter," *IEEE Trans. Signal Process*., vol. 54, no. 11, pp. 4091-4104, Nov. 2006.

[32] R. Mahler, "PHD filters of higher order in target number", *IEEE Trans. Aerosp. Electron. Syst*., vol. 43, no. 4, pp. 1523-1543, Oct. 2007.

[33] B.-T. Vo, B.-N. Vo, A. Cantoni, "Analytic implementations of the cardinalized probability hypothesis density filter," *IEEE Trans. Signal Process*., vol. 55, no. 7, pp. 3553-3567, July 2007.

[34] B.-T. Vo and B.-N. Vo, "Labeled random finite sets and multi-object conjugate priors," *IEEE Trans. Signal Process*., vol. 61, no. 13, pp. 3460-3475, July 2013.

[35] B.-N. Vo; B.-T. Vo, D. Phung, "Labeled random finite sets and the Bayes multi-target tracking filter," *IEEE Trans. Signal Process*., vol. 62, no. 24, pp. 6554-6567, Dec. 2014.

[36] S. C. Nardone, V. J. Aidala, "Observability criteria for bearings-only target motion analysis," *IEEE Trans. Aerosp. Electron. Syst*., vol. 17, no. 2, pp. 162-166, Mar. 1981.

[37] S. C. Nardone, A. G. Lindgren, K. F. Gong, "Fundamental properties and performance of conventional bearings-only target motion analysis," *IEEE Trans. Autom. Control*, vol. 29, no. 9 pp. 775-787, Sep. 1984.

[38] C. Jauffret, D. Pillon, "Observability in passive target motion analysis," *IEEE Trans. on Aerosp. and Electron. Syst*., vol. 32, no. 4, pp. 1290-1300, Oct. 1996.

[39] R. Mahler, *Statistical Multisource-Multitarget Information Fusion*, Artech House, 2007.

[40] B.-N. Vo, S. Singh, A. Doucet, "Sequential Monte Carlo methods for multi-target filtering with random finite sets," *IEEE Trans. Aerosp. Electron. Syst*., vol. 41, no. 4, pp. 1224–1245, Oct. 2005.

[41] B.-T. Vo, B.-N. Vo, A. Cantoni. "The cardinality balanced multi-target multi-Bernoulli filter and its implementations", *IEEE Trans. Signal Process*., vol. 57, no. 2, pp. 409-423, Feb. 2009.

[42] R. Mahler, "Objective functions for Bayesian control-theoretic sensor management, I: Multitarget first-moment approximation," *Proc. IEEE Aerosp. Conf*., Mar. 2003.

[43] A. Logothetis, A. Isaksson, R. Evans, "An information theoretic approach to observer path design for bearings-only tracking," *Proc. 36th Conf. Decision and Control*, San Diego, CA, USA, December 1997.

[44] S. S. Singh, N. Kantas, B.-N. Vo, A. Doucet, R. J. Evans, "Simulation-based optimal sensor scheduling with application to observer trajectory planning," *Automatica*, vol. 43, no. 5, pp. 817-830, May 2007.

[45] X. Wang, M. Morelande, B. Moran, "Sensor scheduling for bearings-only tracking with a single sensor," *Proc. 5th Int. Conf. on Intelligent Sensors, Sensor Networks and Information Processing*, Melbourne, Victoria, Australia, Dec. 2009.

[46] O. Tremois, J. P. Le Cadre, "Optimal observer trajectory in bearings-only tracking for manoeuvring sources," *IEE Proc., Radar, Sonar Navigation*, vol. 146, no. 1, pp. 31–39, February 1999.

[47] D. Schumacher, B.-T. Vo, B.-N. Vo, "A consistent metric for performance evaluation of multi-object filters," *IEEE Trans. Signal Process*., vol. 56, no. 8, pp. 3447–3457, Aug. 2008.

[48] M. Beard, B.-T. Vo, B.-N. Vo, "Bayesian multi-target tracking with merged measurements using labelled random finite sets," *IEEE Trans. on Signal Process*., vol. 63, no. 6, pp. 1433-1447, Mar. 2015.